Environmental Science & Technology

Article

pubs.acs.org/est

Sediment Trapping by Dams Creates Methane Emission Hot Spots

Andreas Maeck,*[,∥] Tonya DelSontro,[†] Daniel F. McGinnis,[‡,∥,&] Helmut Fischer,[§] Sabine Flury,[¶,&] Mark Schmidt,[‡] Peer Fietzek,[‡,⊥] and Andreas Lorke[∥]

[∥]Institute for Environmental Sciences, University of Koblenz-Landau, 76829 Landau, Germany

[†]Swiss Federal Institute of Aquatic Science and Technology, Eawag, 6047 Kastanienbaum, Switzerland and Institute of Biogeochemistry and Pollutant Dynamics, ETH, 8092 Zurich, Switzerland

[‡]GEOMAR Helmholtz Centre for Ocean Research, RD2 Marine Biogeochemistry, 24148 Kiel, Germany

[∥]Nordic Center for Earth Evolution (NordCEE), Institute of Biology, University of Southern Denmark, 5230 Odense M, Denmark

[§]Federal Institute of Hydrology (BfG), 56068 Koblenz, Germany

[¶]Department of Bioscience, Center for Geomicrobiology, Aarhus University, 8000 Aarhus C, Denmark

[⊥]CONTROS Systems and Solutions GmbH, 24148 Kiel, Germany

ABSTRACT: Inland waters transport and transform substantial amounts of carbon and account for ~18% of global methane emissions. Large reservoirs with higher areal methane release rates than natural waters contribute significantly to freshwater emissions. However, there are millions of small dams worldwide that receive and trap high loads of organic carbon and can therefore potentially emit significant amounts of methane to the atmosphere. We evaluated the effect of damming on methane emissions in a central European impounded river. Direct comparison of riverine and reservoir reaches, where sedimentation in the latter is increased due to trapping by dams, revealed that the reservoir reaches are the major source of methane emissions (~0.23 mmol CH_4 m^{-2} d^{-1} vs ~19.7 mmol CH_4 m^{-2} d^{-1}, respectively) and that areal emission rates far exceed previous estimates for temperate reservoirs or rivers. We show that sediment accumulation correlates with methane production and subsequent ebullitive release rates and may therefore be an excellent proxy for estimating methane emissions from small reservoirs. Our results suggest that sedimentation-driven methane emissions from dammed river hot spot sites can potentially increase global freshwater emissions by up to 7%.

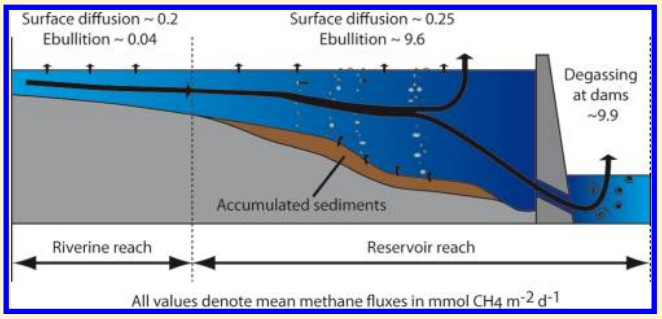

INTRODUCTION

Inland waters are significant sources of the atmospheric greenhouse gases carbon dioxide (CO_2) and methane (CH_4).[1,2] While microbial degradation of organic matter in oxic sediments mainly produces CO_2, anaerobic pathways, e.g. in freshwater sediments, also produce CH_4. Methane released to the atmosphere has a 25 times higher global warming potential than CO_2 per mass on a 100 year time scale;[3] therefore, a shift in the degradation pathway in sediments from aerobic to anaerobic increases the climatic impact of the aquatic system.

River segmentation and disruption by dams changes the suspended particle and bedload transport and leads to the accumulation of sediments in the basins upstream of dams.[4,5] Since settling particles build up cohesive sediment layers, the sediments at high deposition zones (i.e., forebays of dams, sidebays) are frequently anoxic.[4] Worldwide, over 50,000 large dams (storage height > 15 m) and millions of smaller impoundments exist, which has resulted in a reduction of terrestrial organic carbon flux to the ocean by 26% and a storage of 83−250 Tmol (1−3 Pg) of carbon in these reservoirs.[5]

Ultimately, the combination of two important factors - 1) the continuous trapping of both allochthonous and autochthonous organic material in reservoirs, and 2) increased CH_4 production via anaerobic degradation of organic carbon in reservoir sediments - leads to the hypothesis that reservoirs emit significant amounts of CH_4 to the atmosphere.[6]

Quantitative estimates of methane emissions from reservoirs have mainly been obtained for large systems. In the initial phase after construction of the reservoirs, freshly inundated biomass is the major source of methanogensis, while during the aging of the reservoirs, deposited sediment containing organic carbon becomes more important.[7] However, the zones of sedimentation of allochthonous material that enter the reservoir via river inflows are relatively small compared to the large surface area. In small reservoirs, e.g. impounded rivers, the zones of sediment deposition cover a larger fraction of the reservoir's surface area and sediment accumulation rates can be very high.

Received: January 27, 2013
Revised: May 16, 2013
Accepted: June 25, 2013

   dx.doi.org/10.1021/es4003907 | Environ. Sci. Technol. XXXX, XXX, XXX−XXX

Small reservoirs are particularly susceptible to intense sedimentation, which is supported by the observation that rapid sediment accumulation reduces the water storage capacity of small reservoirs faster than large reservoirs.[8] The rapid sedimentation with high organic loads typically leads to anaerobic environments that are ideal for active methanogenesis if the organic substrate is available. Despite the hypothesized high areal emission rate, studies of CH_4 emissions from small reservoirs are rare. Therefore, the thrust of this study are (1) to test the hypothesis that small reservoirs in impounded rivers that trap large amounts of organic carbon have high CH_4 emission rates, and (2) to provide a quantitative analysis of the factors regulating CH_4 emissions and emission pathways in these systems.

Measurements were performed over a 93-km section of the River Saar (Germany) that includes six small-sized reservoirs (<1 km^2) and the intermediate riverine reaches between the dams. All relevant emission pathways, including diffusive surface emissions, degassing at dams, and bubble-mediated transport, were quantified continuously over the entire longitudinal transect using sensor measurements for dissolved CH_4 and hydroacoustics to determine bubble emissions. High spatial resolution sediment accumulation data coupled with measured ebullition rates revealed a quantitative relationship between sediment accumulation and CH_4 bubble flux. By upscaling our results, using a rough estimate of the global areal extent of impounded river sections, we assess their potential impact on atmospheric CH_4 budgets.

MATERIAL AND METHODS

Study Site. The Saar River flows from its source in the French Vosges mountains along 246 km through France and Germany. The lower 96 km within Germany were impounded between 1976 and 2000 for cargo ship transport purposes. Six dams with ship-locks and hydropower plants were installed to increase the minimum depth to at least 4 m within the main channel. We use the official nomenclature in kilometers from the confluence with the River Moselle (river-km) to denote locations along the river. The damming of the Saar led to elongated water residence times, lower flow velocities, and to increased water depths.[9] Simultaneous to the river impoundment, the construction of wastewater treatment plants in the catchment area helped to improve the water quality of the Saar[10] (for physicochemical parameters see Table 1). In summer, however, oxygen levels can still drop below 125 μM, especially in the forebays of the dams where organic rich cohesive sediments accumulate.[10] Upstream of these areas, the river bed is characterized by gravel and stones. Macrophytes were absent within the main channel but were frequent in connected shallow side bays during the period of our survey.

Table 1. Physico-Chemical Parameters of the River Saar[a]

parameter	value/range
ammonia	7−35 μM NH_4^+-N
nitrate	136−271 μM NO_3^--N
ortho-phosphate	3−11 μM ortho-PO_4^{3-}-P
total organic carbon	242−700 μM C
chemical oxygen demand	278−756 μM O_2 d^{-1}
temperature	2−25 °C
discharge	18 m^3 s^{-1} MNQ/76 m^3 s^{-1} MQ/526 m^3 s^{-1} HQ_1
catchment area	7431 km^2

[a]Chemical parameters were measured in 2010 (n =13) at station Fremersdorf (km 48). Data were provided by the International Commission for the Protection of the Moselle and the Saar, www.iksms-cipms.org. Discharge data refer to the period 1953 to 2002.

Sampling Summary. The measurement campaign was conducted from the fifth to the 11th of September 2010. We equipped a boat with a CH_4 sensor, an echosounder system, and a multiparameter probe to measure the dissolved concentration of CH_4, bubble occurrence and associated flux rates, and supporting water quality parameters, respectively. Data were obtained along the entire 93 km stretch of the German river reach which includes six reservoirs and their intermediate reaches. In the forebays, we sampled along zigzag transects, while in the remaining sections, measurements were performed along the longitudinal river axis. Water and sediment samples were taken while underway. To include seasonal variability, we conducted stationary measurements of ebullition rates at selected locations during six campaigns between June 2011 and January 2012.

Sediment Accumulation. Riverbed elevation data were provided by the Water and Shipping Agency Saarbruecken. A specialized survey vessel equipped with 36 sonar transducers on side arms measures the height of the riverbed annually with an accuracy of ±10 cm. The geographic position of each measurement point is determined using differential GPS. Cross-sectional transects were measured every 100 m in the year 1993 and every 25 m in the following years. To calculate the net sediment accumulation rate, we subtracted the data sets position of the riverbed surface of 1993 from 2010 and divided the value by 17 years. The data were interpolated using anisotropic kriging following a coordinate transformation according to Merwade et al.[11] The geographic position was converted into longitudinal and lateral coordinates since most riverine processes show a strong anisotropy along the direction of flow. The large input data set allowed calculating variograms, which were further used for anisotropic kriging. To include the anisotropy due to the longitudinal flow direction, the search angles were set to ±30°, and the search distance in the longitudinal direction was approximately 10 times the search distance in the lateral direction. After kriging on a 1 × 1 m grid for the zones where gas bubbles were detected and a 5 × 5 m grid for the remaining sections, the data were then transformed back into geographic coordinates.

Sediment Analysis. Sediment cores were taken at sites with soft sediments in the impoundments Saarbruecken, Lisdorf, Rehlingen, and Serrig (1, 1, 1, and 5 cores, respectively) using a piston corer. The cores were analyzed for porosity, organic carbon content, and porewater CH_4 concentration. For CH_4, 4 mL of sediment was sampled with cutoff syringes and immediately transferred to crimp capped 20 mL vials containing 4 mL of 2.5% NaOH solution for conservation. Porewater samples were taken at several depths from the upper 20 cm below the sediment-water interface (SWI). The concentration in the headspace of the vials was measured using gas-chromatography. Porosity and organic carbon content were determined in three samples per core.

The diffusive flux from the sediment into the water column $J_{diffusive,\ SWI}$ [mol CH_4 m^{-2} d^{-1}] was calculated as

$$J_{diffusive,\ SWI} = \phi \times D_{CH4,sed} \times \frac{\Delta C_{porewater}}{\Delta z} \quad (1)$$

dx.doi.org/10.1021/es4003907 | Environ. Sci. Technol. XXXX, XXX, XXX−XXX

where ϕ refers to the porosity [-]. The diffusivity of CH_4 in the sediment porewater, $D_{CH4,sed}$ [m^2 d^{-1}], was taken from Schulz and Zabel[12] and corrected for the effect of tortuosity according to Boudreau.[13] The gradient of the change in CH_4 concentration $\Delta C_{porewater}$ [mol m^{-3}] over the depth interval Δz [m] within the sediment was calculated by fitting a linear regression over the linear section of the porewater profile. R^2-values ranged from 0.79 to 0.96, indicating that the assumption of a linear gradient is fulfilled.

Diffusive Surface Emissions. Dissolved CH_4 concentrations were logged continuously in 1 m water depth using a Contros HydroC methane sensor, based on membrane equilibration and infrared sprectrometry. Water samples for sensor calibration and validation were taken every kilometer for laboratory analysis of dissolved CH_4 following Bastviken et al.[14] Bottles sealed with a butyl stopper were evacuated, flushed with N_2, and evacuated again. To create a defined headspace, 20 mL of N_2 was added. For preservation, 250 μL of H_2SO_4 and $CuCl_2$ was added. In the field, a Ruttner sampler was used for water sampling and connected to the prepared bottles so that the water was transferred from the sampler to the bottles by the vacuum inside the bottles. The previously injected 20 mL of N_2 created the headspace in the bottle. Since water samples were collected in 1 m depth, the pressure reduction by bringing the sampler to the surface is negligible, thus errors due to degassing of the samples as described in Fearnside et al.[15] cannot occur. Headspace gas was analyzed using a gas chromatograph equipped with a flame-ionization detector. The headspace-CH_4 concentration was converted to the water concentration using the relation of Bossard et al.[16] All water samples were analyzed within four weeks after sampling. The agreement between sensor-based *in situ* measurements and dissolved CH_4 concentrations in the samples was reasonable (linear regression, $R^2 = 0.77$, $p < 0.0001$, $n = 54$). Deviations can be attributed to the relatively long response time of the sensor ($t_{63} \sim 10$ min) as opposed to the real-time character of the discrete samples. Compared to the gas chromatography measurements the factory calibrated sensor readings possessed a mean offset of -0.065 μM with a standard deviation of 0.1 μM.

Diffusive atmospheric fluxes of methane J_{diff} [mol CH_4 m^{-2} d^{-1}] were estimated from measured concentrations of dissolved gas C_W [mol CH_4 m^{-3}] using the boundary layer equation

$$J_{diff} = k \times (C_w - C_{eq}) \tag{2}$$

where C_{eq} [mol CH_4 m^{-3}] is the atmospheric equilibrium concentration at a given temperature. C_{eq} was calculated using Henry's law with the Henry coefficient from Dean[17] and an atmospheric concentration of 1.8 ppm. The gas exchange velocity k [m d^{-1}] was calculated as a function of wind speed using the empirical relationship by Crusius et al.[18] Since flow velocities were usually far below 0.3 m s^{-1} and the depth was always > 2 m, it is likely that the wind dominated the near-surface turbulence, and thus k.[19,20] However, downstream of dams, the flow velocity and turbulence were strongly enhanced, and we estimated these emissions as described below (degassing at dams).

To identify the transport pathways leading to changes in the CH_4 concentration along the river, we used a mass balance approach to determine the required import of CH_4 into the water column. The CH_4 import

$$J_{CH4,import} = (C_{out} - C_{in}) \times \frac{d \times v}{l} + J_{CH4,WAI} \tag{3}$$

where C_{in} and C_{out} [M] are the CH_4 concentrations at the inflowing and outflowing boundary, d [m] is the water depth, v [m d^{-1}] is the average flow velocity, l [m] is the length between inflowing and outflowing boundary, and $J_{CH4,WAI}$ [mol CH_4 m^{-2} d^{-1}] is the sink term due to diffusive surface emissions.

Degassing at Dams. The concentration of dissolved CH_4 was used to estimate the degassing emission at the dams, $J_{degassing}$ [mol CH_4 m^{-2} d^{-1}] as the product of the concentration difference between up- (C_{up}) and downstream (C_{down}) [mol CH_4 m^{-3}] of the dam and discharge Q [m^3 d^{-1}]:

$$J_{degassing} = (C_{up} - C_{down}) \times Q \tag{4}$$

Since discharge was measured in Fremersdorf (km 48), it was scaled according to the size of the catchment area to obtain more accurate results for the individual dams.

Bubble Flux Emissions. A Simrad EY60 scientific echosounder equipped with a split-beam elliptical transducer (120 kHz, 10° × 4° beam angle) was mounted to the boat to vertically record echograms throughout the survey for bubble detection. The echogram bubble analysis was performed using Sonar 5 Pro software (Lindem Acquisition, Norway) and restricted to the water layer between the sediment surface and 2.9 m below the transducer to avoid error due to target detection in the transducers near-field zone. Distinction between bubbles and fish or other nonbubble targets was made based on rise velocity v_z [m s^{-1}], where bubbles rise at speeds between 0.1 and 0.35 m s^{-1}, and fish have a vertical v_z less than 0.1 m s^{-1}. Echograms were also checked visually, and all unknown targets were erased manually. The remaining bubbles were used for flux analysis, which is based on the procedure described in Ostrovsky et al.[21] and DelSontro et al.[22] The estimated acoustic target strengths of individual bubbles were converted to volume using the following relationship

$$V = 2.76 \times 10^5 \times e^{0.295 \times TS} \tag{5}$$

where V [mL] is the volume of the bubble, and TS is acoustic target strength [dB]. TS is a log representation of the acoustic backscattering cross-section of a target, σ_{bs} [m^2], which is the variable measured via an echosounder ($TS = 10 \times log_{10}(\sigma_{bs})$). Equation 5 was derived by a calibration conducted at 10 m depth in a natural lake, where CH_4 gas bubbles of known volume were released while the echosounder recorded from above, using a similar procedure as described in Ostrovsky et al.[21]

The concentration of gas bubbles per scanned water volume $C_{bubbles}$ [m^3 m^{-3}] was determined by

$$C_{bubbles} = \frac{\sum_i V_i}{V_{scanned\ water}} \tag{6}$$

where V_i refers to the volume of bubble i [m^3], and $V_{scanned\ water}$ [m^3] was calculated using the volume equation of a truncated cone with the transducer beam angles and the length of the transect. Ebullition rates J_{bubble} [m^3 CH_4 m^{-2} d^{-1}] were estimated as the product of bubble volume concentration $C_{bubbles}$, bubble rise velocity v_z, and fraction of CH_4 within the bubble C_{CH4} [-]

$$J_{bubbles} = C_{bubble} \times v_z \times C_{CH4} \tag{7}$$

and afterward converted to moles CH_4 per m^2 and day by using the ideal gas law. For determining the relationship between ebullition- and sediment accumulation rate, the bubble flux rate was calculated for 5 s long intervals. For every sediment

dx.doi.org/10.1021/es4003907 | Environ. Sci. Technol. XXXX, XXX, XXX−XXX

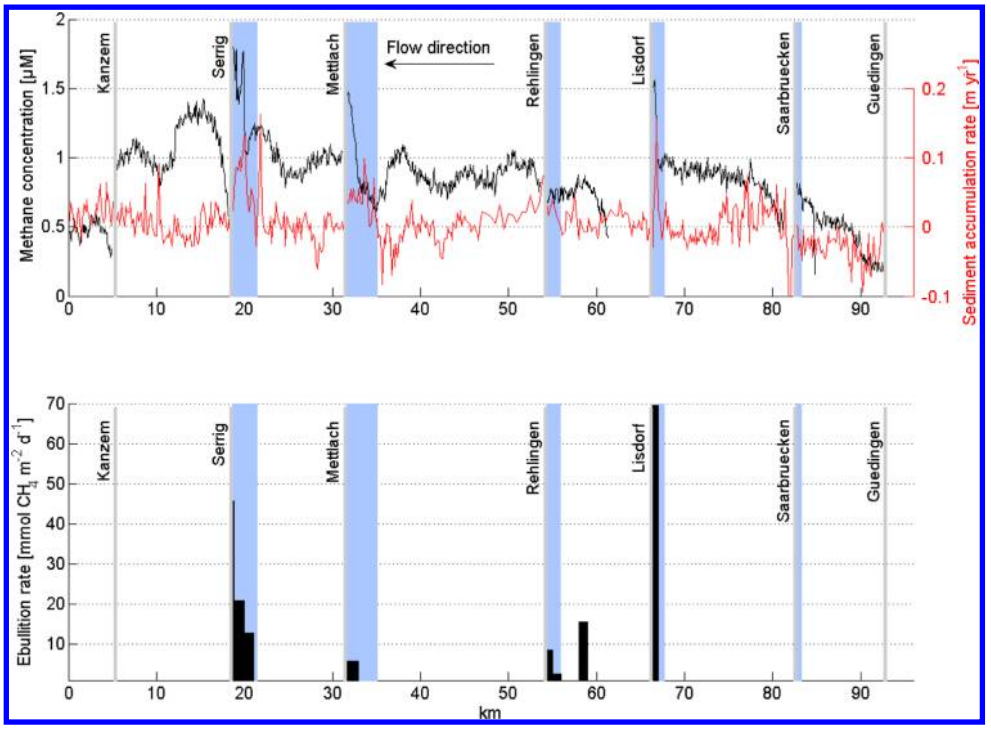

Figure 1. Concentration of dissolved CH_4 and average sediment accumulation rate per cross-section (upper panel) and ebullition rate (lower panel, black bars) along the River Saar in km distance from the confluence with the River Moselle. Vertical gray lines mark the locations of dams labeled by their name. The reservoirs zones are marked in blue.

accumulation rate interval from −0.15 to 0.3 m yr^{-1}, the mean of all ebullition rate measurements was calculated. A linear regression analysis was performed using the log-transformed ebullition rate and the sediment accumulation rate (between the years 1993 and 2010). Using this relationship (see Results section: eq 8), we estimated the ebullition rate $J_{bubble,sr}$ [mmol CH_4 m^{-2} d^{-1}] for entire zones where bubbles were detected, based on the sediment accumulation rate data.

Seasonal Ebullition Measurements. Funnel-shaped gas traps were deployed at five sites in the basin Serrig (between km 19.3 and km 20.1, water depth: 2.5 to 4 m) during six campaigns from June 2011 until January 2012. The gas traps consist of inverted funnels with diameters of 60 or 100 cm that caught rising bubbles in a cylindrical container. Filling height was measured to determine the volume of the captured gas, while gas chromatographic analysis revealed its CH_4 concentration. A deployment time of between 8 and 24 h ensured to account for subdaily variations.

RESULTS

Sediment Characterization and Accumulation. Along the entire transect, the riverbed consisted of varying sediment types ranging from coarse material (stones and rocks) to fine-grained cohesive particles. In the forebays, the sediment was mainly soft, fine-grained and organic-rich, while further upstream of the dams, the riverbed tended toward stony to rocky material. At sites with soft sediments, core samples showed a mean porosity of 0.8 ± 0.04 (range: 0.74 to 0.86) and an organic carbon content of 5.8 ± 0.8% (range: 4.5 to 6.9%).

Analyzing bathymetric data over several years show that the strongest sediment accumulation occurred in the forebays (Figure 1, Figure 2). The net sediment accumulation rate for the 17-year period between 1993 and 2010 ranged from −0.05

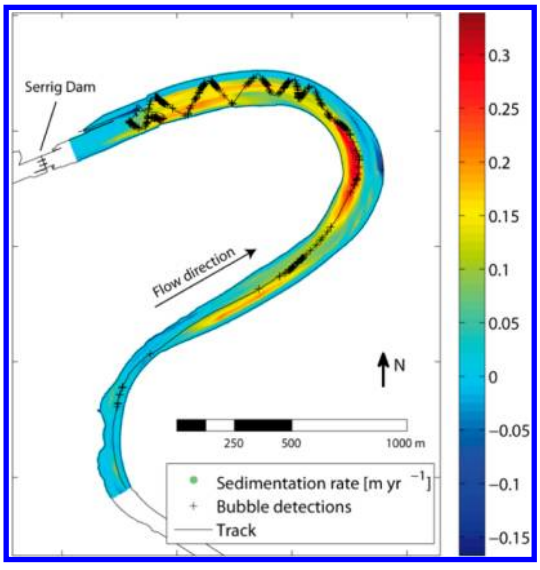

Figure 2. Mean sediment accumulation rate between 1993 and 2010 (color scaling) and bubble detections in the forebay of Serrig dam. Crosses mark bubble detection along the sampling transect, which is denoted by the black line.

m yr^{-1} in areas characterized by erosion up to > 0.35 m yr^{-1} at sediment deposition zones.

Sediment-Water Column CH_4 Flux. Sediment porewater in the forebays was strongly supersaturated with CH_4, and bubbles were observed in the sediment cores starting between 5 and 10 cm below the SWI (Figure 3). Calculated diffusive fluxes from the sediment into the water column ranged from 2.2 to 4.7 mmol CH_4 m^{-2} d^{-1} with an average of 3.4 ± 1.1 mmol CH_4 m^{-2} d^{-1}. One sediment core taken close to the upper gate of the locking chamber Serrig (km 18.7) showed a

dx.doi.org/10.1021/es4003907 | Environ. Sci. Technol. XXXX, XXX, XXX−XXX

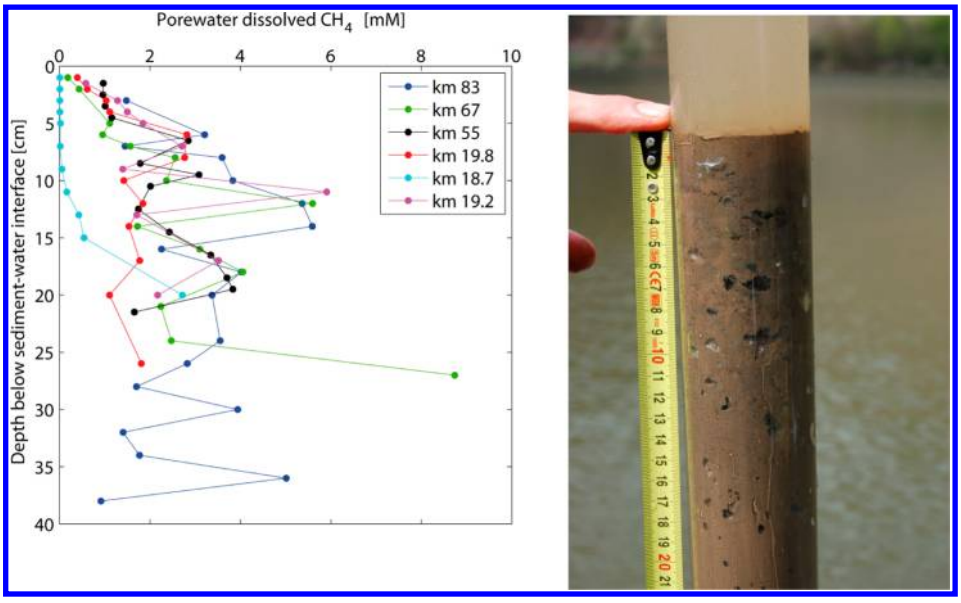

Figure 3. Dissolved CH_4 concentrations in the porewater of six sediment cores (left side). The core at km 18.7 (light blue line) shows that methanogenesis starts deeper, presumably due to ship-induced resuspension of the upper layer. On the right side, the photograph of a sediment core sampled in the Serrig basin shows the presence of free gas.

Table 2. Ebullition Rates Measured in the Serrig Impoundment Using Funnel-Shaped Gas Traps

	ebullition rate [mmol CH_4 m^{-2} d^{-1}]					
sampling site	June 2011	Aug 2011	Sept 2011	Nov 2011	Jan 2012	mean ± std
km 19.4	185	73	92	8	169	105 ± 72
km 19.7	291	14	481	4	0	158 ± 219
km 19.9	494	219	522	87	0	264 ± 236
km 20.05	221	41	356	77	16	142 ± 144
km 20.15	1764	4	237	11	7	87 ± 111
mean ± std	273 ± 131	70 ± 87	338 ± 177	37 ± 41	38 ± 73	-

shift of the CH_4 profile to a greater depth, most likely due to frequent resuspension caused by passing ships.

Dissolved CH_4. Dissolved CH_4 concentrations showed a clear pattern along the river beginning with an increase in the first two impoundments from 0.1 μM to a base level of ~1 μM (Figure 1). In the downstream impoundments, concentrations were quite variable, but regularly increased by up to ~0.5 μM km^{-1} in the forebays, and were often followed by a sharp drop in the tailwaters of the dams. The increase of dissolved CH_4 toward the dams results from an import of CH_4 into the water column, and, hence, the mass balance approach from Equation 3 was used to quantify the magnitude of the import. For example, the increase of 0.42 μM between km 20 and 19 requires an import of 10.4 mmol CH_4 m^{-2} d^{-1}.

Diffusive Surface Emissions. The Saar River water was supersaturated with CH_4 by a factor of 260 to 780 compared to atmospheric equilibrium. Areal rates of diffusive surface gas exchange with the atmosphere ranged from 0.02 to 0.48 mmol CH_4 m^{-2} d^{-1} (mean, 0.21 mmol CH_4 m^{-2} d^{-1}) during the survey. Total diffusive emissions for the entire river surface of this study (6.49 km^2) was 1,400 mol CH_4 d^{-1}.

Degassing Emissions at Dams. High CH_4 concentrations upstream and lower concentrations downstream of dams revealed a substantial loss of dissolved CH_4 to the atmosphere. Despite representing a much smaller surface area compared to the diffusive flux across the entire river surface, dam degassing emissions $J_{degassing}$ (Equation 4) ranged between 400 and 3,800 mol CH_4 d^{-1} for the different dams. Total dam loss was approximately 10,000 mol CH_4 d^{-1}.

Emissions via Gas Bubbles. The zones of elevated dissolved CH_4 near the dams overlap with zones of high sediment accumulation rates and intense ebullition (Figure 1). Bubbles were only detected at sediment deposition sites upstream of dams and at the inlet of the tributary Prims at km 58 (Figure 1, Figure 2). Bubbles varied in size with radii ranging from 0.4 to 12.6 mm and a mean of 2.8 ± 1.2 mm. Average ebullition rates for 1-km-long segments ranged from 0.63 to 68.8 mmol CH_4 m^{-2} d^{-1} (Figure 1). The ebullitive fluxes varied strongly both spatially and temporally (Figure 1, Table 2).

A correlation analysis between the measured ebullition flux along the ship-track and local sediment accumulation rates revealed a strong relationship between both parameters. Observed ebullitive emissions increased exponentially with the corresponding sediment accumulation rates and led to a highly significant relationship (R^2 = 0.91; p < 0.001; n = 7, Figure 4). Using the sediment accumulation rate SR_i from each grid cell i [m yr^{-1}] as a proxy for the ebullition rate $J_{bubble,sr}$ [mmol CH_4 m^{-2} d^{-1}], the ebullition−sedimentation relationship

$$J_{bubble,\,sr} = \sum 2.4 \times e^{17.9 \times SR_i} \quad (8)$$

was applied to the entire surface area of zones where bubbles were observed. Thus, areas of observed ebullition and extensive sedimentation emitted approximately 12,700 mol CH_4 d^{-1} via

dx.doi.org/10.1021/es4003907 | Environ. Sci. Technol. XXXX, XXX, XXX−XXX

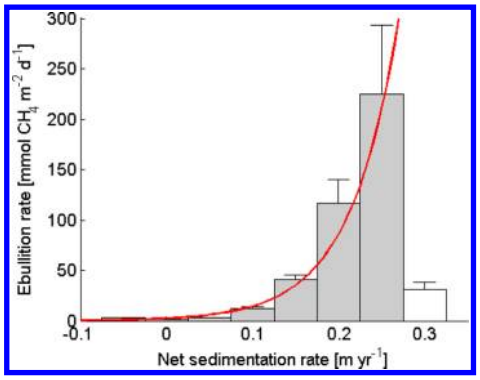

Figure 4. Relationship between sediment accumulation rate (1993–2010) and measured ebullition rates. The red line shows the exponential fit (R^2 = 0.91; p < 0.001; n = 7). The white bar at 0.3 was excluded from the analysis due to its small sample size. Error bars denote the standard error of mean.

ebullition. The river-type reaches of the Saar, which did not accumulate sediment as extensively as the forebays, only emitted 190 mol CH_4 d^{-1} via ebullition.

Seasonal Ebullition Measurements. Ebullition rates, measured using funnel-shaped gas traps in the Serrig impoundment, showed a seasonal pattern with lower emissions during colder periods and higher emissions during the summer months (Table 2). Individual measurements ranged from 0 up to 522 mmol CH_4 m^{-2} d^{-1}. The mean bubble flux rates of the five measurement sites ranged per site from 87 to 264 mmol CH_4 m^{-2} d^{-1}. Measured CH_4 concentrations in the collected gas ranged from 71 vol.-% to 90 vol.-% with a mean of 84.5 ± 5.8 vol.-%.

Comparison Between Reservoirs and Intermediate Sections. For further analysis, the entire river stretch was divided into reservoir and river-type (or intermediate) reaches distinguished by the steep increase in river width toward the forebays. We estimated the mean bubble flux rate based on the relationship of Equation 8 within the reservoir reaches where ebullition was observed to be 9.6 mmol CH_4 m^{-2} d^{-1} (individual reservoir values in Table 3). Combined with surface diffusion and dam degassing, the mean CH_4 flux for the reservoir reaches ranged from 4.7 to 38.6 mmol CH_4 m^{-2} d^{-1} (mean: 19.7 mmol CH_4 m^{-2} d^{-1}), while the river-type reaches emit 0.23 mmol CH_4 m^{-2} d^{-1}, a factor of 80 less (Table 3).

DISCUSSION

Sediment Accumulation Determines Methane Emissions. Over 90% of the CH_4 emissions from the entire 96-km of the Saar are from the reservoir sections which cover only ~16% of the total surface area. In these hot spot emission zones, large amounts of sediments accumulate and lead to the enrichment of CH_4 in the water and subsequent evasion to the atmosphere via the release of CH_4 gas bubbles.

The relationship between sediment accumulation rate and ebullition provides the direct link between the deposition of organic matter and CH_4 ebullition along the Saar. A similar relationship has been observed by Sobek et al.[23] in the highly methanogenic sediments of a Swiss hydropower reservoir (Wohlensee). The authors propose that if the carbon burial rate exceeds the rate of carbon mineralization, then highly reactive carbon is readily available for microbes in deeper sediment layers.[23] The ebullition-sediment accumulation relationship obtained for the Saar is based on the average net sediment accumulation rate over a 17-year period, and the nonlinear increase of ebullitive emissions with sedimentation reveals that deeper sediment layers also contribute to CH_4 formation.

To compare the sediment-accumulation-ebullition relationship with another system, we applied it to the Wohlensee reservoir (mean sedimentation rate 0.78 m yr^{-1}).[23] Our relationship (Eq. 8) predicts a flux rate of 9.63 mmol CH_4 m^{-2} d^{-1}, which is in very close agreement with the average emission rate of 9.38 mmol CH_4 m^{-2} d^{-1} that is reported for this reservoir.[24] This extremely close agreement in estimates suggests that the derived relationship is not site-specific but may also be applied to other temperate reservoirs having comparable sediments with respect to their CH_4-productivity.

CH_4 Transport Pathways. In the River Saar, CH_4 is transported from the sediments to the atmosphere by three major pathways: surface diffusion, degassing at dams, and ebullition.

The observed increase in dissolved CH_4 within the dam forebays can be attributed to enhanced transport of CH_4 from the sediments into the water column. Diffusive transport from the sediments into the water column is too low to explain the high CH_4 rise toward the dams. As well, since microbial CH_4 oxidation at the SWI can be expected to be a strong sink for upward diffusing CH_4, the transport via diffusion will be substantially reduced.[25] The transport of CH_4 from bubbles to the ambient water ("bubble dissolution"), on the other hand, can explain the observed pattern of dissolved CH_4 in the forebays, assuming that ~10% of the bubble CH_4 dissolves.[26] There can be additional CH_4 transport mechanisms occurring in the River Saar, such as bubble-, ship-, or wave-enhanced porewater release.[27,28]

Since the source of dissolved CH_4 is methanogenic sediment most prevalent in the forebays, the diffusive and dam degassing

Table 3. Emissions per Reservoir and Pathway

		diffusive emissions		ebullition		degassing at dams	total emissions	areal flux
reservoir[a]	area [km^2]	[mol CH_4 d^{-1}]	[mmol CH_4 m^{-2} d^{-1}]	[mol CH_4 d^{-1}]	[mmol CH_4 m^{-2} d^{-1}]	[mol CH_4 d^{-1}]	[mol CH_4 d^{-1}]	[mmol CH_4 m^{-2} d^{-1}]
Serrig	0.38	136	0.36	10,431	27.4	4037	14,604	38.6
Mettlach	0.39	88	0.23	878	3.0	1355	2321	6.0
Rehlingen	0.17	29	0.18	357	2.0	401	787	4.7
Lisdorf	0.06	15	0.29	966	7.1	1135	2116	34.7
Saarbrücken	0.04	7	0.21	no bubbles observed		615	622	14.4
river-type reach between reservoirs	5.49	1,068	0.2	188	0.04	-	1263	0.23

[a]Please note that the Kanzem dam is not included here since the channel-like geometry of the basin does not allow a separation into reservoir and river reach. Sediment accumulation in this reservoir reach was negligible.

dx.doi.org/10.1021/es4003907 | Environ. Sci. Technol. XXXX, XXX, XXX–XXX

emissions are also linked to sediment accumulation. The magnitude of both flux pathways increases with increasing dissolved CH_4 concentrations. Water discharge at the dams, either through ship locks or turbines, is associated with enhanced turbulence, mixing and pressure variations that locally accelerate diffusive exchange with the atmosphere. Therefore, both variables describing the diffusive transport, namely the concentration gradient and the gas transfer velocity, increase at the dams, leading to higher emissions compared to surface diffusion at the river-type sections.

Ebullition with its dual effects, the direct transport of CH_4 from the sediments to the atmosphere and the dissolution of rising bubbles with a subsequent enrichment of dissolved CH_4 in the water column, was the dominant transport pathway. Measured ebullition rates within the longitudinal survey fit well with seasonal gas trap measurements; however, ebullition rates showed strong seasonal variability with lower values during the winter, and higher fluxes associated with higher water temperatures (Table 2). This relationship may reflect the temperature dependence of methane production and solubility. Temperatures during the longitudinal survey in September 2010 ranged between 13 and 14 °C, which is the approximate annual mean water temperature in the Saar. However, since the temperature dependence of emissions can be nonlinear[24] and thus, fluxes throughout periods with high temperatures can be disproportionately high, our estimate based on the data from the basin-scale survey potentially underestimates seasonally averaged emission rates.

While the major source of CH_4 in other reservoirs could also be the accumulation of organic-rich sediment, the contribution from the emitting pathways could be different to that of the River Saar. For example, in deep reservoirs, bubble dissolution during ascent and subsequent oxidation in the water column will result in lower bubble-mediated emission rates.[26] However, if CH_4 oxidation is low, e.g. due to an anoxic hypolimnion, the dissolved CH_4 may accumulate in the water column. This stored CH_4 may then be emitted to the atmosphere via other pathways, such as by degassing at the dam outflow or further downstream[29] or deep convective mixing and turnover.[30]

IMPLICATIONS

Previous research has found that temperate reservoirs and rivers emit less than 1.3 mmol CH_4 m^{-2} d^{-1}.[2,7,31] The mean CH_4 emission rate from reservoir reaches of the temperate River Saar (19.7 mmol CH_4 m^{-2} d^{-1}) exceeds this estimate by more than one order of magnitude and falls in the range of emissions previously reported for tropical reservoirs.[2,7]

To evaluate the potential CH_4 emissions from hot spot zones in river systems on a global scale, the global surface area of rivers from Downing et al.[32] (360,627 km^2) was used along with the finding from Nilsson et al.,[33] that 59% of all large river systems are affected by dams. Furthermore, we assumed that 15% of the surface area of affected rivers constitute reservoir zones, and that the emission rates are within the observed limits of 4.7 and 38.6 mmol CH_4 m^{-2} d^{-1} (Table 3) (mean emission rate of the Saar reservoirs and Wohlensee: 18 mmol CH_4 m^{-2} d^{-1}). These rough estimates show that hot spots in river impoundments can emit globally between 56 and 450 Gmol CH_4 yr^{-1}, which corresponds to 0.9 and 7.2 Tg CH_4 yr^{-1} (mean: 0.21 Gmol yr^{-1} or 3.4 Tg CH_4 yr^{-1}) or an increase of 0.8% to 7% (mean 3.3%) of the current estimate of global freshwater CH_4 emissions[2]. However, the uncertainty in this estimate is large as the area estimate includes only larger rivers (>100 m breadth), no reliable data of the affected surface area of impoundments are available, and CH_4 emission rates of other impounded rivers are severely lacking. This is especially important for dammed rivers in the tropics, which contribute 49% of the global surface area of rivers and where high temperatures potentially accelerate the degradation of organic matter, consequently increasing CH_4 emission rates. On a global scale, the construction of new dams, especially in systems where damming causes significant retention of carbon, is most likely associated with an increase in CH_4 emissions from aquatic systems.

Regarding the net emissions of sediment-trapping dams, the life-cycle of accumulating sediments must be taken into account.[34] If a fraction of the buried carbon remains unavailable for microbial degradation, then sedimentation basins could also act as a carbon sink despite their high CH_4 emissions. However, in many cases, particularly in reservoirs in impounded rivers, sediments are dredged to maintain navigation and prevent turbine blockage or river meandering. The dredged material is often released downstream, followed by sedimentation at the next dam. Thus, long-term burial of carbon at sediment trapping dams is often prevented, and a large fraction of the carbon is presumably emitted from the aquatic system either as CO_2 or CH_4.

In summary, sediment accumulation in deposition zones, such as dam forebays, fuels high CH_4 emissions that can account for a large proportion of the total CH_4 evasion from the entire aquatic system. In the case of the River Saar, sediment accumulation accounts for over 90% of the CH_4 emissions, and most of the CH_4 is transported from the sediments to the atmosphere by rising gas bubbles. Ultimately, ebullition measurements are crucial for quantifying aquatic CH_4 emissions from this type of aquatic system but also many others. The coupling of ebullition measurements with sedimentation data can thus be a powerful tool to estimate basin-scale emissions. Areal emission rates of the Saar reservoirs exceed reported CH_4 emissions from temperate reservoirs by one order of magnitude, pointing toward a strong contribution from sediment-trapping dams to global CH_4 emissions. As the number of dams worldwide continues to increase and sediments further accumulate behind already established impoundments, the contribution from CH_4 emissions from hot spots to global atmospheric CH_4 levels is also likely to increase in the future, especially when coupled with higher average temperatures.

AUTHOR INFORMATION

Corresponding Author

*Phone: +49 6341 280 31573. E-mail: maeck@uni-landau.de

Present Address

[&]Leibniz-Institute of Freshwater Ecology and Inland Fisheries, 12587 Berlin, Germany.

Notes

The authors declare the following competing financial interest(s): There are no competing financial interests of all authors except of P. Fietzek, who is affiliated with the company Contros, the manufacturer of the methane sensor used in this study. Since we validated the sensor measurements with gas-chomatography analysis of water samples at the University of Koblenz-Landau, the objectivity of our results is ensured.

■ ACKNOWLEDGMENTS

We would like to thank to the Water and Shipping Agency Saarbrücken for their support during our surveys as well as for data supply and to Osman Ghamraoui for support regarding the postprocessing analysis of the HydroC data. Furthermore, we would like to thank Florian Burgis for his help during the survey and Bernd Mockenhaupt for support with the echosounder device.

The manuscript was written through contributions of all authors. All authors have given approval to the final version of the manuscript. A. Maeck, A. Lorke, D. F. McGinnis, S. Flury, T. DelSontro, and H. Fischer participated at the sampling campaign. A. Maeck, M. Schmidt, and H. Fischer analyzed samples in the laboratory and A. Maeck, A. Lorke, T. DelSontro, and P. Fietzek analyzed the data. Writing the manuscript was done by A. Maeck, A. Lorke, D. F. McGinnis, S. Flury, and T. DelSontro. All authors commented on the manuscript. This study was financially supported by the German Research Foundation (grant LO 1150/5-1).

■ REFERENCES

(1) Cole, J.; Prairie, Y.; Caraco, N.; McDowell, W.; Tranvik, L.; Striegl, R.; Duarte, C.; Kortelainen, P.; Downing, J.; Middelburg, J. Plumbing the global carbon cycle: integrating inland waters into the terrestrial carbon budget. *Ecosystems* **2007**, *10* (1), 172−185.

(2) Bastviken, D.; Tranvik, L. J.; Downing, J. A.; Crill, P. M.; Enrich-Prast, A. Freshwater methane emissions offset the continental carbon sink. *Science* **2011**, *331* (6013), 50.

(3) Forster, P.; Ramaswamy, V.; Artaxo, P.; Berntsen, T.; Betts, R.; Fahey, D. W.; Haywood, J.; Lean, J.; Lowe, D. C.; Myhre, G. Changes in atmospheric constituents and in radiative forcing. *Clim. Change* **2007**, 20.

(4) Kennedy, R. H.; Walker, W. W. Reservoir nutrient dynamics. *Reservoir limnology: Ecological perspective*; Wiley: 1990.

(5) Syvitski, J. P. M.; Vörösmarty, C. J.; Kettner, A. J.; Green, P. Impact of humans on the flux of terrestrial sediment to the global coastal ocean. *Science* **2005**, *308* (5720), 376−380.

(6) Giles, J. Methane quashes green credentials of hydropower. *Nature* **2006**, *444* (7119), 524−525.

(7) Barros, N.; Cole, J. J.; Tranvik, L. J.; Prairie, Y. T.; Bastviken, D.; Huszar, V. L. M.; Del Giorgio, P.; Roland, F. Carbon emission from hydroelectric reservoirs linked to reservoir age and latitude. *Nat. Geosci.* **2011**, *4* (9), 593−596.

(8) Glymph, L. M. Summary: sedimentation of reservoirs. *Geophys. Monogr. Ser.* **1973**, *17*, 342−348.

(9) Schöl, A. Die Saar - Auswirkungen der Stauregelung auf den Sauerstoffhaushalt in einem abflussarmen Mittelgebirgsfluss. In *Staugeregelte Flüsse in Deutschland*; Friedrich, Günther Kinzelbach, Ragnar: Stuttgart, 2006; pp 170−187.

(10) Becker, A.; Kirchesch, V.; Baumert, H. Z.; Fischer, H.; Schöl, A. Modelling the effects of thermal stratification on the oxygen budget of an impounded river. *River Res. Appl.* **2010**, *26* (5), 572−588.

(11) Merwade, V.; Cook, A.; Coonrod, J. GIS techniques for creating river terrain models for hydrodynamic modeling and flood inundation mapping. *Environ. Modell. Softw.* **2008**, *23* (10−11), 1300−1311.

(12) Schulz, H. D.; Zabel, M. *Marine geochemistry*; Springer: 2007.

(13) Boudreau, B. P. *Diagenetic models and their implementation*; Springer: Berlin, 1997; Vol. *505*.

(14) Bastviken, D.; Cole, J.; Pace, M.; Tranvik, L. Methane emissions from lakes: Dependence of lake characteristics, two regional assessments, and a global estimate. *Global Biogeochem. Cycles* **2004**, *18* (4), GB4009.

(15) Fearnside, P. M.; Pueyo, S. Greenhouse-gas emissions from tropical dams. *Nat. Clim. Change* **2012**, *2* (6), 382−384.

(16) Bossard, P.; Joller, T.; Szabó, E. Die quantitative Erfassung von Methan im Seewasser. *Schweiz. Z. Hydrol.* **1981**, *43* (1), 200−211.

(17) Dean, J. A. *Lange's handbook of chemistry*; 1985.

(18) Crusius, J.; Wanninkhof, R. Gas transfer velocities measured at low wind speed over a lake. *Limnol. Oceanogr.* **2003**, 1010−1017.

(19) Maeck, A.; Lorke, A. Ship-lock-induced surges in an impounded river and their impact on subdaily flow velocity variation. *River Res. Appl.* **2013**, DOI: 10.1002/rra.2648.

(20) Alin, S. R.; de Fátima F. L. Rasera, M.; Salimon, C. I.; Richey, J. E.; Holtgrieve, G. W.; Krusche, A. V.; Snidvongs, A. Physical controls on carbon dioxide transfer velocity and flux in low−gradient river systems and implications for regional carbon budgets. *J. Geophys. Res.: Biogeosci.* **2011**, *116*, G1.

(21) Ostrovsky, I.; McGinnis, D. F.; Lapidus, L.; Eckert, W. Quantifying gas ebullition with echosounder: the role of methane transport by bubbles in a medium-sized lake. *Limnol. Oceanogr.: Methods* **2008**, *6*, 105−118.

(22) DelSontro, T.; Kunz, M. J.; Kempter, T.; Wüest, A.; Wehrli, B.; Senn, D. B. Spatial heterogeneity of methane ebullition in a large tropical reservoir. *Environ. Sci. Technol.* **2011**, *45* (23), 9866−9873.

(23) Sobek, S.; DelSontro, T.; Wongfun, N.; Wehrli, B. Extreme organic carbon burial fuels intense methane bubbling in a temperate reservoir. *Geophys. Res. Lett.* **2012**, *39* (1), L01401.

(24) DelSontro, T.; McGinnis, D. F.; Sobek, S.; Ostrovsky, I.; Wehrli, B. Extreme methane emissions from a Swiss hydropower reservoir: contribution from bubbling sediments. *Environ. Sci. Technol.* **2010**, *44* (7), 2419−2425.

(25) Liikanen, A.; Martikainen, P. J. Effect of ammonium and oxygen on methane and nitrous oxide fluxes across sediment−water interface in a eutrophic lake. *Chemosphere* **2003**, *52* (8), 1287−1293.

(26) McGinnis, D.; Greinert, J.; Artemov, Y.; Beaubien, S.; Wüest, A. Fate of rising methane bubbles in stratified waters: How much methane reaches the atmosphere? *J. Geophys. Res.: Oceans* **2006**, *111*, C9.

(27) Hofmann, H.; Federwisch, L.; Peeters, F. Wave-induced release of methane: Littoral zones as a source of methane in lakes. *Limnol. Oceanogr.* **2010**, *55* (5), 1990−2000.

(28) Lorke, A.; McGinnis, D. F.; Maeck, A.; Fischer, H. Effects of ship locking on sediment oxygen uptake in impounded rivers. *Water Resour. Res.* **2012**, DOI: 10.1029/2012WR012483.

(29) Fearnside, P. M. Do hydroelectric dams mitigate global warming? The case of Brazil's Curuá-Una Dam. *Mitigation Adaptation Strategies Global Change* **2005**, *10* (4), 675−691.

(30) López Bellido, J.; Tulonen, T.; Kankaala, P.; Ojala, A. CO2 and CH4 fluxes during spring and autumn mixing periods in a boreal lake (Pääjärvi, southern Finland). *J. Geophys. Res.: Biogeosci.* **2009**, *114*, G4.

(31) St. Louis, V. L.; Kelly, C. A.; Duchemin, É.; Rudd, J. W. M.; Rosenberg, D. M. Reservoir surfaces as sources of greenhouse gases to the atmosphere: A global estimate. *BioScience* **2000**, *50* (9), 766−775.

(32) Downing, J. A.; Duarte, C. M. Abundance and Size Distribution of Lakes, Ponds and Impoundments. In *Encyclopedia of Inland Waters*; Gene, E. L., Editor-in-Chief; Academic Press: Oxford, 2009; pp 469−478.

(33) Nilsson, C.; Reidy, C. A.; Dynesius, M.; Revenga, C. Fragmentation and flow regulation of the world's large river systems. *Science* **2005**, *308* (5720), 405−408.

(34) Mendonca, R.; Kosten, S.; Sobek, S.; Barros, N.; Cole, J. J.; Tranvik, L.; Roland, F. Hydroelectric carbon sequestration. *Nat. Geosci.* **2012**, *5* (12), 838−840.